RESEARCH ARTICLE

Deviating from the Norm: Peculiarities of *Aplysia cf. californica* Early Cleavage Compared to Traditional Spiralian Models

YOLANDA E. CHÁVEZ-VITERI[1,2], FEDERICO D. BROWN[2,3,4,5], AND OSCAR D. PÉREZ[1]*

[1]Laboratorio de Biología del Desarrollo 113, Escuela de Ciencias Biológicas, Pontificia Universidad Católica del Ecuador, Quito, Ecuador
[2]Centro Nacional de Acuicultura e Investigaciones Marinas, Escuela Politécnica del Litoral, San Pedro, Santa Elena, Ecuador
[3]Evolutionary Developmental Biology Laboratory, Department of Biological Sciences, Universidad de los Andes, Bogotá, Colombia
[4]Departamento de Zoologia, Instituto de Biociências, Universidade de São Paulo, São Paulo, SP, Brazil
[5]Instituto Nacional de Ciência e Tecnologia em Estudos Interdisciplinares e Transdisciplinares em Ecologia e Evolução (IN-TREE), Salvador, BA, Brazil

ABSTRACT

Spiralia represents one of the main clades of bilaterally symmetrical metazoans (Bilateria). This group is of particular interest due to the remarkable conservation of its early developmental pattern despite of the high diversity of larval and adult body plans. Variations during embryogenesis are considered powerful tools to determine ancestral and derived characters under a phylogenetic framework. By direct observation of embryos cultured in vitro, we analyzed the early cleavage of the euopisthobranchs *Aplysia cf. californica.* We used tubulin immunocytochemistry to stain mitotic spindles during early cleavages, and followed each division with the aid of an autofluorescent compound inside yolk platelets, which differed from the characteristic pink-brownish pigment of the vegetal cytoplasm in zygotes and early embryos. We found that this species exhibits an unequal cleavage characterized by ooplasmic segregation, oblique inclination of mitotic spindles, and differences in size and positioning of the asters in relation to the cellular cortex. Furthermore, we detected asynchrony in cleavage timing between the two large macromeres C and D, which increases the number of cleavage rounds required to reach a particular cell stage in comparison to other spiralians. Here, we report the presence of a transient and previously

Grant sponsor: Pontificia Universidad Católica del Ecuador: Grant number: PUCE L-13238; Grant sponsor: Universidad de Los Andes; Grant sponsor: Secretaría Nacional de Ciencia, Tecnología e Innovación (Senescyt-Ecuador).

Additional Supporting Information may be found in the online version of this article.

*Correspondence to: Oscar D. Pérez, Laboratorio de Biología del Desarrollo 113, Escuela de Ciencias Biológicas, Pontificia Universidad Católica del Ecuador, Apartado 17-01-2184, Avenida 12 de Octubre 1076 y Roca, Quito 170517, Ecuador.
E-mail: odperez@puce.edu.ec

Received 9 April 2016; Revised 8 September 2016; Accepted 3 October 2016
DOI: 10.1002/jez.b.22718
Published online 29 December 2016 in Wiley Online Library (wileyonlinelibrary.com).

undescribed U-shaped embryo in this species. The present detailed description of *A. californica* early development deviates considerably from stereotypical patterns described in other spiralians. Our observations demonstrate that early spiralian development can be more plastic than previously thought. *J. Exp. Zool. (Mol. Dev. Evol.) 328B:72–87, 2017.* © 2016 Wiley Periodicals, Inc.

J. Exp. Zool. (Mol. Dev. Evol.) 328B:72–87, 2017

How to cite this article: Chávez-Viteri YE, Brown FD, Pérez OD. 2017. Deviating from the norm: Peculiarities of *Aplysia cf. californica* early cleavage compared to traditional spiralian models. J. Exp. Zool. (Mol. Dev. Evol.) 328B:72–87.

The spiral cleavage is a stereotypical pattern that was first described more than a century ago (Conklin, 1897). Typically, it consists of diagonal cell divisions obliquely aligned with respect to the animal–vegetal (AV) axis. The first two cleavages occur along the AV axis; as a result, a first quartet of cells is spawned, which are conventionally identified as macromeres A–D (Conklin, 1897). Among all, the blastomere D is suggested to mark the future lateral dorsal side of the embryo (Martindale, '86; Shimizu et al., 2014). Later, a set of four smaller blastomeres is generated toward the animal pole. These cells, known as micromeres, are labeled with a lower case letter that represents the mother cell (macromere) from which they arise, and a number preceding that letter, symbolizing the quartet to which they belong. Therefore, the first quartet of micromeres will consist of a set of small blastomeres known as 1a–1d. Subsequently, a second quartet of micromeres is generated from the macromeres (2a–2d). During this division, the mitotic spindles are shifted in the opposite direction of the first quartet of macromeres, oriented either clockwise or counter clockwise, around the main embryonic axis (AV axis). This generates an oblique alternating arrangement of cells, which is consecutively followed by succeeding cellular divisions, resulting in a classic holoblastic spiral configuration (Costello and Henley, '76).

Remarkably, some lophotrochozoan taxa exhibit variations in the formation of early blastomeres, differing from the traditional spiral cleavage described above. These deviations have been identified in several groups such as Rotifers, Platyhelminthes, Nemerteans, Molluscs, and Annelids (Lambert, 2010; Adell et al., 2015; Bleidorn et al., 2015; von Döhren, 2015; Wanninger and Wollesen, 2015). The promoting mechanisms that differ among taxa are generally established during the first two cellular divisions (Goldstein and Freeman, '97; Henry and Martindale, '99; Henry, 2014). For example, the leech *Helobdella robusta* exhibits unequal early cleavage, which is driven by differences in the polarization of the two mitotic spindles during metaphase prior the first cleavage, with one of the spindle poles expanding toward the cortex, while the other one shrinks, losing most of its microtubules. These processes promote the uneven cytokinesis that generates two unequal size blastomeres, one large (CD) and another small (AB) (Ren and Weisblat, 2006). In addition, unequal cleavage could also be driven by the formation of a "polar lobe", a vegetal anucleate bulge produced as a result of the asymmetric segregation of cytoplasmic materials inherited by one cell. Particularly, this phenomenon has been broadly documented in molluscs and annelids, where the polar lobe usually is generated during the first two cell divisions (Clement, '52; Dohmen, '83; Henry et al., 2006; Lambert, 2008). Generally, the formation of a polar lobe is a dynamic process of cytoplasmic migration that generates changes in the shape of the embryo, resulting in different morphologies such as L-shaped, trilobed-, or calabash-shaped embryos, among others (Yin et al., 2013). Moreover, the asymmetric division of the early embryos is not necessarily produced or limited to one specific mechanism; in fact, some species, such as the polychaete *Chaetopterus variopedatus,* achieve unequal cleavage throughout the combination of both, unequal cytokinesis due to a spindle shift and polar lobe formation (Henry, '86).

As exemplified before, the mechanisms that generate asymmetries in spiralians can differ among organisms. Thus, the conservation or divergence of specific developmental modes, body patterns, and axis determinants are considered important characters to establish phylogenetic relationships, underlining the interplay between ontogenesis and evolution (Palmer, '96; van den Biggelaar and Haszprunar, '96; Hejnol, 2010). An early phylogenetic meta-analysis of developmental modes in spiralians examined several embryological features such as cleavage patterns, mechanisms of D-quadrant determination, and larvae morphology; the authors concluded that unequal cleavage might be a derived condition (Freeman and Lundelius, '92). However, further studies based on fossil and living molluscs have suggested that symmetrical cleavage patterns may have derived from asymmetrical/unequally cleaving ancestors (Dzik, '99; Vermeij, 2002). Regardless of when developmental asymmetries first arose during the evolution of spiralians, extant taxa show that unequal cleavage occurs in several clades.

Unequal cleavage in the Euopisthobranchia, commonly known as sea hares and sea slugs, shows a remarkable variation in cleavage patterns and general developmental modes, including the occurrence of poecilogony (i.e., intraspecific variation of development) that occurs in only a few groups of invertebrates (Chia et al., '96; Krug, '98). Although the traditional spiralian equal cleavage, as exhibited by the cephalaspidean *Haminoea callidegenita* (Boring, '89), is the common pattern described in euopisthobranchs, there are also reports of deviations

from that typical developmental mode (Saunders, '10; Heyland et al., 2011; Lee et al., 2014). In some euopisthobranchs, a polar lobe is formed by cytoplasmic segregation that generally occurs after the first and second cleavage. The lobe is a temporary structure that is either small and unnoticeable, or very conspicuous with remarkably large amounts of pigment, as in the nudibranch *Madrella sanguinea* (Page, 2007). While diverse cleavage patterns have been reported in euopisthobranchs, so far there is no general consensus on which type of cleavage should be considered ancestral and their evolutionary and ecological implications.

In this study, we examine and compare the embryogenesis of two euopisthobranch species, *Aplysia cf. californica* (hereafter referred to simply as *A. californica,* Order: Anaspidea) and *Navanax aenigmaticus* (Order: Cephalaspidea). The development of *A. californica* in early and late stages has been described previously (Heyland et al., 2011; Vue et al., 2014); yet, the cellular mechanisms driving it is less known. In contrast, factors such as distribution, morphology, and taxonomy of *N. aenigmaticus* are well known (Camacho-Garcia et al., 2005; Ornelas-Gatdula et al., 2012); however, there are no current reports on their embryogenesis.

This research aims to unveil cellular processes leading to variations in early development of *N. aenigmaticus* and *A. californica*. In order to get a cellular understanding of cleavage differences between these two species, we recorded the dynamics of cytological constituents, such as ooplasmic segregation and shifts in the disposition of the mitotic spindles. Our study aims to draw attention to the high variation of early developmental modes observed within Spiralia.

MATERIALS AND METHODS

Animal Collection and Culture

Adult specimens of an aplysiid, tentatively identified as *A. californica*, were collected from tide-pools in Ballenita, Prov. Santa Elena, Ecuador (2°12′21.4″S, 80°52′50.98″W) during October, 2012. Animals were removed manually from the intertidal rocky shores during low tide. Rocks from the same habitat that contained the algae *Laurencia* sp. were also taken to the laboratory to feed the *A. californica* adults. There is some question about the name of the species used in this study, as the distribution of *A. californica* has not been confirmed in the southeastern pacific. *Navanax aenigmaticus* specimens were collected in the same locality as *A. californica* (Ballenita). To feed *N. aenigmaticus*, we collected several individuals of *Elysia diomedea* (= Sacoglossa) that were used as prey. Specimens were maintained under controlled conditions in the Laboratory of Developmental Biology at the Pontificia Universidad Católica del Ecuador in Quito. Adults were kept in aquaria with filtered and UV-sterilized seawater at a salinity of 30 ± 1 ppt, under 21 ± 1°C. Oviposition was induced by thermic shock by increasing the temperature to 27°C. Egg ribbons were collected soon after oviposition and kept in separate containers to be photographed and fixed. The early development of 600 living embryos (50 embryos coming from 12 different egg masses) was followed using a compound microscope Carl Zeiss Jenamed 2 (CarlZeiss Inc, NY, USA). Staging of embryos in this study were done using the classic standard nomenclature for spiralian embryos (Conklin, 1897).

Immunocytochemistry

Embryos of both species were manually removed from their capsules using fine Dumont tweezer, 5TI (Electron Microscopy Sciences, PA, USA) and fixed in 4% paraformaldehyde during 12 hr at 4°C. Next, they were rinsed three times every 10 min with Phosphate-buffered Saline (PBS) with Triton or PBT (0.1% Triton-X in PBS) and kept refrigerated long enough for embryos to settle. In order to block nonspecific binding of immunoglobulins, embryos were kept for 60 min in 2 mg/mL of bovine serum albumin in PBT at room temperature (RT). After blocking samples were incubated in a primary antibody raised in rabbit against tubulin (monoclonal antibody 12G10 anti-alpha-tubulin (Developmental Studies Hybridoma Bank, Iowa, USA) diluted in PBT (1:1,000) over night at 4°C. Embryos were washed at RT three times in PBT during 30 min each time. The embryos were incubated in the secondary antibody Alexa fluor 488 anti-rabbit (Invitrogen Thermo Scientific, Waltham, MA USA) in PBT (1:1,000) at RT during 2 hr. To prepare the embryos for the final staining, they were rinsed three times during 10 min in PBT, and one time in PBS during 30 min. Embryos were then incubated at RT for 3 min in the nuclear stain 4′,6-diamidino-2-phenylindole (DAPI) (ThermoFisher Scientific, Massachusetts, USA) diluted in PBS (1:1,000). Finally, they were rinsed for 10 min in distilled water and mounted as shown below.

Microscopy and Image Processing

For in vivo microscopic observations, we placed the embryos in a drop of UV-sterilized seawater on a concave microscope slide. We used plasticine between the slip and slide as spacers to make sure that the embryos were not squeezed or exposed to any pressure by the coverslip. Then, the coverslip was sealed with Vaseline to avoid water evaporation, and water was replaced in the preparation every 4 hr to avoid anoxia. Cell divisions under light microscopy were recorded using a camera Cannon EOS Rebel T1i and software EOS Utility Professional 3.8 (Canon USA Inc, Tokyo, Japan). For fluorescent microscopy, the embryos were placed in a glass slide with two drops of autoclaved glycerol (70%) and placed in dark containers. Documentation of the results was done with an epifluorescent microscope Olympus BX51 attached to a fluorescent Q7 Hg lamp U-LH100 (Olympus Corp, Tokyo, Japan). Filters used and their corresponding excitation wavelengths were as follows: FITC (494 nm), Texas Red (596 nm), and DAPI (350 nm). We also used confocal microscopy using an Olympus FluoView™ FV1000 (Olympus Corp, Tokyo,

Japan) at the Universidad de Los Andes in Bogotá, Colombia. We used the following excitation wavelengths for the confocal: 633 nm (red wavelength) to detect potential autoflorescent molecules, 488 nm (green wavelength) for viewing tubulin, and 385 nm (blue light wavelength) to reveal DAPI. Embryos were documented and processed using Olympus Floview FV10-ASW software (version 04.02.02.09). We used ImageJ and Photoshop version CS6 software to estimate metric features such as size of the blastomeres (mean diameter), size of the platelets (mean surface area), inclination of the mitotic spindle in relation to the equator of the embryo (angle), and distances from the asters to the cortex of the cell (longitude). Finally, the results were tested for statistical significance by performing a two-tailed *t*-test.

RESULTS AND DISCUSSION

Morphology of Egg Masses

Egg ribbons of *A. californica* were laid as long pink or brownish strings containing numerous encapsulated embryos immersed in soft gelatinous material protected by a thick outer membrane (Fig. 1A and a). Each capsule contained 12–15 embryos (Fig. 1a′). The one-cell embryo of *A. californica* was spherical and flattened at the poles, thus the meridional diameter (mean = 89.63 μm, SD = 0.92, n = 8) was smaller than the equatorial diameter (mean = 93.50 μm, SD = 1.16, n = 8) of the embryo. The developmental timing of the embryos within a specific capsule was not synchronized, particularly during the first three cleavages. Some embryos were found at least one stage ahead compared to their siblings. This could be attributed to differences in the timing of fertilization. Previous studies have shown that the time for hatching of larvae within a capsule is related to the early embryonic differences in developmental timing, but is independent of egg/embryo size within the capsules (Jackson et al., 2012). Egg masses of *N. aenigmaticus* consisted of a thin cord of capsules embedded in jelly forming a cylindrical white arrangement (Fig. 1B and b). Each capsule contained a single nonpigmented fertilized embryo (mean = 84.63 μm, SD = 2.84, n = 14) (Fig. 1b′). Among euopisthobranchs, there is a high interspecific variation of the general structure of the egg mass, where features, such as number of embryos per capsule, thickness of the capsule, density, and fine structure of the mucous layers, are the most common variables (Bandel, '76; Klussmann-Kolb and Wagele, 2001; Wilson, 2002). The most remarkable difference between egg masses of *N. aenigmaticus* and *A. californica* was the density and thickness of the outer mucous cover. It has been assumed that this particular structure provides protection to the embryo against infections and other environmental stressors (Benkendorff et al., 2001; Klussmann-Kolb and Wagele, 2001; Przeslawski, 2004; Kaviarasan et al., 2012). Evidence found in previous studies of euopisthobranchs, including antartic species, suggests that the number of protective layers of egg masses could be directly related to the level of environmental stress (Wägele, '96). The difference between the outer mucus cover of egg masses of the two species might be associated with the substrate of the eggs. While egg masses of *A. californica* were usually found under rocks, most egg masses of *N. aenigmaticus,* observed on the field, were laid on macroalgae. Therefore, the high level of exposure of the eggs of *N. aenigmaticus* to environmental and biotic stressors could explain the higher thickness and density of the egg mass cover of this species compared to *A. californica*.

Aplysia californica Early Development

We followed the timing of cell divisions from the one-cell embryo until the gastrula. This analysis showed clear heterochronies in the development among derivatives of the AB lineage versus derivatives of CD.

First Cleavage Forms a U-Shaped Zygotic Stage. Once the eggs were laid but prior to the first cell cleavage, two polar bodies formed at the distant animal pole of the embryo as a result of meiosis. Contrary to previous reports on the development of *A. californica* (Heyland et al., 2011), we found that the polar bodies were visible further than the third cleavage, and at least until the 24-cell stage.

The pigmentation of newly deposited one-cell embryos was uniform, presenting a pink-brownish set of platelets almost equally distributed inside the cell (Fig. 2A and A′). Later, a cap of nonpigmented cytoplasm appeared at the animal pole and started to expand, migrating toward the equatorial midline of the embryo, while the pigmented platelets became segregated to the vegetal side (Fig. 2B and B′). By using brightfield and fluorescent microscopy, we found a stratified cytoplasmic content from the animal to the vegetal poles, exhibiting three different cytoplasmic contents: (i) animal nonpigmented platelets, easily detected under light microscopy at the animal pole, (ii) a thin strand of autofluorescent material composed of numerous small platelets (surface area: mean = 5.07 μm^2, SD = 0.95, n = 10) at the equatorial region of the embryo, and (iii) a lighter, autofluorescent and less concentrated pigmented constituent composed of big platelets (surface area: mean = 14.73 μm^2, SD = 2.16, n = 10) at the vegetal side. Previous studies of fluorescent microscopy of mollusk embryos and larvae reported the presence of autoflorescent yolk platelets (Croll, 2006; Sandenbergh and Roodt-Wilding, 2012), but we have now identified the presence of at least two distinct autofluorescent components leading to the stratification of the cytoplasm described above. The spectral characteristics of these unknown components were excited at green and red wavelengths. Our results suggest that the autoflorescent compounds are restricted to the platelets and seem to be completely independent from the visible pink-brownish pigment of the embryos. It is likely that the two different autofluorescent platelets could correspond to the fatty yolk (small platelets) and the proteid yolk (far vegetal big platelets),

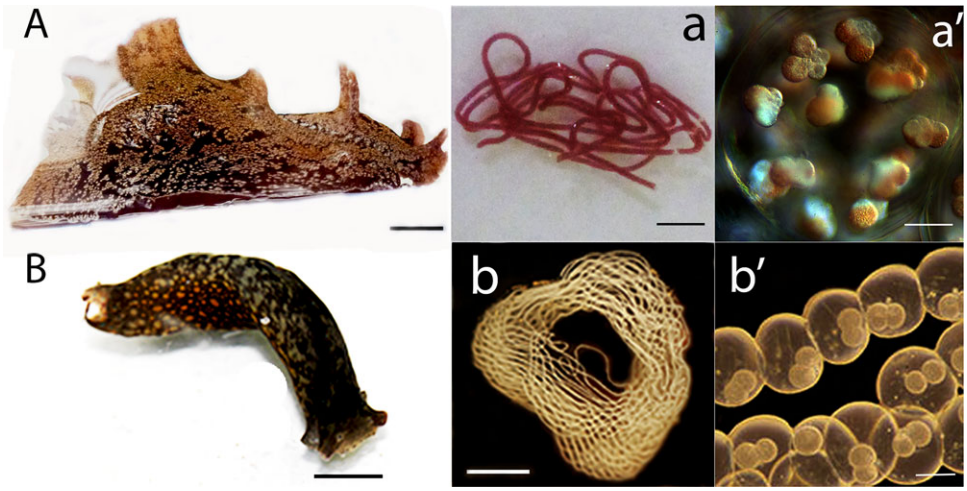

Figure 1. Adults and egg masses of *Aplysia californica* and *Navanax aenigmaticus*. (A) *Aplysia californica* adult; (a) *A. californica* egg mass consists of a long string with encapsulated pink-brownish embryos immersed in a gelatinous tissue and protected by a thick membrane; (a′) *A. californica* capsules contain 12–15 embryos; (B) *N. aenigmaticus* adult; (b) *N. aenigmaticus* egg mass is white and cylindrical, and consist of a thin cord of capsules embedded in jelly; (b′) *N. aenigmaticus* capsules contain one single embryo. Scale bars: 2 cm in (A), 0.5 cm in (a), 100 μm in (a′), 1 cm in (B), 0.50 cm in (b), 100 μm in (b′). [Color figure can be viewed at wileyonlinelibrary.com]

as previously described by developmental studies on *Aplysia limacine* (Raven, '58). Nevertheless, further biochemical analyses are required to confirm this assumption.

After the zygotic cytoplasm became clearly stratified, two processes occurred in parallel during the first asymmetric cell division: (1) ooplasmic rearrangement, first observed due to the peculiar pigmentation of platelets found in this species, and (2) ooplasmic segregation as a result of an asymmetric and oblique constriction of the embryo close to its midline, perpendicular to the AV axis (Fig 2C and C′). Subsequently, a transient stage of cleavage produced a U-shaped embryo (Fig. 2D–F′, Fig. S2) that lasted 20 min, which could be easily missed if embryogenesis was not carefully monitored. The U-shaped stage ended after the first cleavage furrow was completed. The opposite asymmetrical furrow appeared on the pigmented side, opposite to the polar bodies, and expanded obliquely with respect to the AV axis leading to a redistribution of the cytoplasm (Fig. 2G and G′). It would be interesting to explore whether these asymmetries in the cleavage furrow are generated by displaced elements of the cytoskeleton with respect to the cellular cortex or by unequally deposited inhibitory signals from astral microtubules (Canman, 2009; Von Dassow et al., 2009). Previous studies have recognized astral and central spindle microtubules as drivers of furrowing (Glotzer, 2004; D'Avino et al. 2005). Unfortunately, the descriptive nature of our study did not allow us to clearly evaluate these hypotheses, but future in vitro manipulations of centrosomes, nuclei, and microtubules could clarify the main players that generate cleavage asymmetries in the spiralians.

After the cleavage furrow completed its progression, cells underwent a compaction phenomenon (i.e., maximization of adhesive cell contacts (Gilbert, 2014)) likely promoted by an increased tension from the outer surface of the embryo, rather than by cell adhesion (Maître et al., 2015). The two polar bodies remained at the animal pole, and the pigmented platelets continued to segregate toward the vegetal pole of the large blastomere. Finally, a two-celled embryo was formed that contained two asymmetric blastomeres: the large blastomere (prospective CD) mostly containing pigmented platelets and the smaller blastomere (prospective AB) that was nearly pigment free (Fig. 2H and H′).

Colored embryos and ooplasmic segregation have been reported before for other euopisthobranchs (Bandel, '76; Wilson, 2002; Page, 2007). For instance, during early cleavage of the nudibranch *M. sanguinea* red-orange pigmented yolk platelets migrate vegetally and a pigmented polar lobe is formed during second cleavage that remains visible in the embryo until the gastrula stage (Page, 2007). However, a transitory U-shaped embryo has not been described before in *A. californica* or any other species within the group Euopisthobranchia. This peculiar morphology of the U-shaped embryo during the first cleavage could erroneously suggest the presence of a presumptive polar lobe, however fluorescent DNA markers revealed the presence of nuclei in each of the two bulges observed besides the obliquely forming cleavage furrow. Thus, we discarded a possible presence of a polar lobe and confirmed the assumption that the unusual U-shaped embryo is in fact a consequence of a reorganization

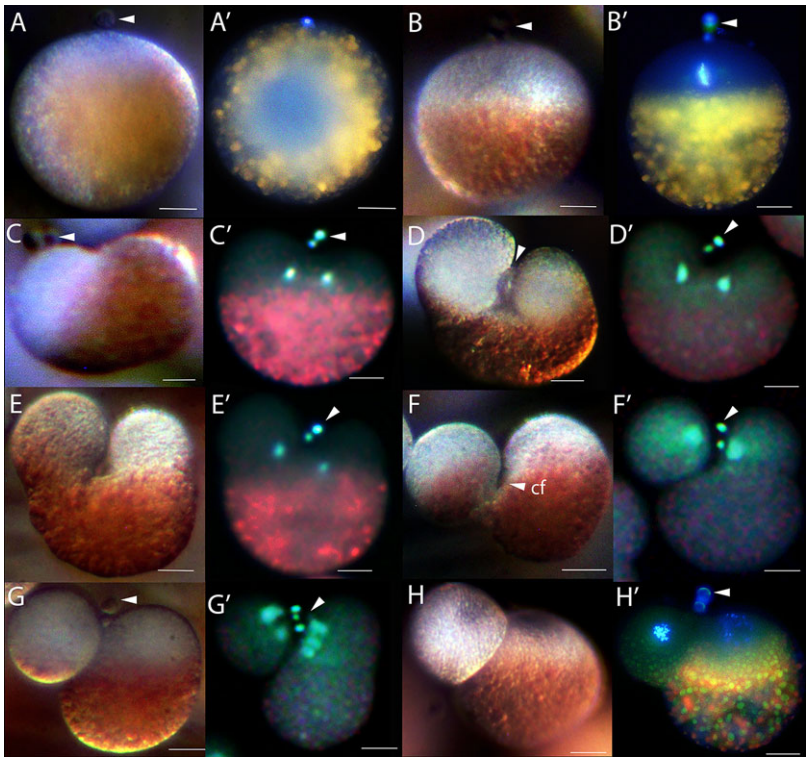

Figure 2. *Aplysia californica* first cleavage, ooplasmic segregation, and formation of temporary U-shaped embryo. (A) Newly deposited one-cell embryo presents a uniform pigmentation; (B) one-cell stratified embryo; (C) beginning of ooplasmic segregation; the pigmented yolk platelets are confined to the vegetal pole of the embryo while the animal pole remains almost free of yolk; (D) a small constriction is formed perpendicular to the animal–vegetal axis; the polar bodies (arrow heads) are visible at the point where the cleavage furrow first develops; (E) the constriction occurs at a nonstrictly middle point, a cleavage furrow that expands toward the interior of the embryo becomes evident, and the cytoplasm is rearranged; (F) progressively a U-shaped embryo is formed; (G) complete cytokinesis results in a two-cell stage embryo with blastomeres of different size, and the cleavage furrow (cf) disappears; (H) as cytokinesis is completed, the resulting two blastomeres adhere to each other tightly. (A′–H′) Nuclei are shown by blue fluorescence and pigmented yolk platelets by red autofluorescence of the embryos at different stages. Scale bars: 20 μm. [Color figure can be viewed at wileyonlinelibrary.com]

of cytoplasmic constituents. We did not find evidence of polar lobe formation at any other stage of development in *A. californica*. The unusual ooplasmic segregation reported here for *A. californica* (i.e., the formation of the U-shaped embryo stage) is likely associated with embryonic axial patterning crucial to properly distribute morphogenetic determinants along the AV axis of early embryos as shown in other gastropods (Freeman, 2006).

Second Cleavage is Asynchronous and Gives Rise to the Prospective D-Quadrant. Second cleavage was asynchronous and generated a transient intermediate stage of a three-cell embryo. The AB blastomere divided perpendicularly to the AV axis and produced two symmetric daughter cells, that is, small macromeres A and B. Cytokinesis during second cleavage was rapidly followed by cell compaction mechanisms that attached the small macromeres tightly to the CD macromere, which remained undivided. The pigmented yolk was uniformly distributed inside the CD macromere, whereas the new blastomeres A and B did not carry any pigmented cytoplasm (Fig. 3A and A′). The highly pigmented blastomere (CD) divided unequally and perpendicular to the AV axis, producing a big presumptive D macromere (mean diameter = 50.41 μm, SD = 0.65, n = 12) and a smaller C macromere (mean diameter = 45.50 μm, SD = 1.42, n = 12), both containing small and big pigmented yolk platelets (Fig. 3B and B′).

In unequal-cleavers the D-quadrant has been postulated to be the largest cell, but size alone cannot be reliably used for D-quadrant identification in equal-cleavers. The D-quadrant can be identified in some species by other criteria related to spatial

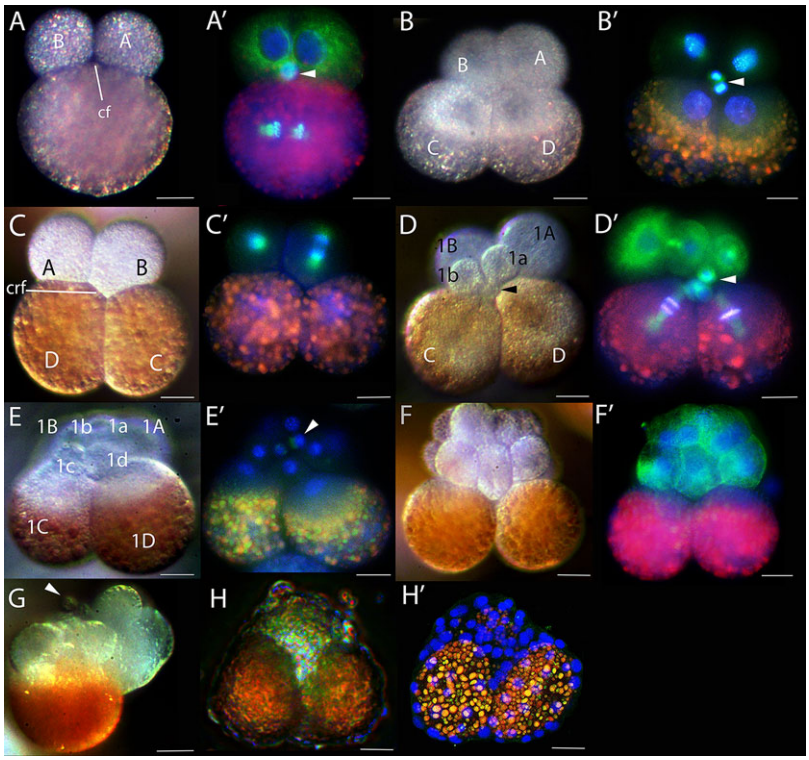

Figure 3. Atypical asynchronous and asymmetric early cleavage of *Aplysia californica* from three-cell stage onwards. (A) Animal view of the embryo during the three-cell stage. (A′) The mitotic spindle situates at a nonstrict middle point of the cell. (B) Four-cell embryo animal view; two asymmetric large macromeres C and D are produced. (C) Vegetal view of the embryo in four-cell stage; the largest macromere (presumptive D blastomere) has the highest number of cell contacts at the cross-furrow. (D) Six-cell embryo animal view; the daughter cells of the macromeres A and B (1a and 1b) are released in direction to the animal pole. (E) Eight-cell embryo animal view; the micromeres produced by macromeres C and D (1c and 1d) complete the formation of the first tetrad. (F) Vegetal view of the embryo in 24-cell stage. (G) Lateral view of the 24-cell embryo; micromeres are generated through asynchronous alternate cell divisions produced in oblique angles toward the animal pole of the embryo. (H) Heart-shaped gastrula and gastrulation occurs through epiboly. The micromeres migrate to the surface and surround the two still distinguishable large yolky macromeres. Some platelets are found outside the macromeres, which are mainly concentrated in the posterior end of the embryo that corresponds to the future blastopore. The presence of the two polar bodies (arrow heads) denotes the animal side of the embryos. (A′-H′) Microtubules are shown by green immunofluorescence, nuclei by blue fluorescence and pigmented yolk platelets by red autofluorescence. Scale bars: 20 μm. [Color figure can be viewed at wileyonlinelibrary.com]

positioning or blastomere interactions, such as highest number of contacts of the putative D-blastomere (Goulding, 2003). In *A. californica* embryos, the cross-furrow at the four-cell stage was asymmetrically positioned, and therefore not all blastomeres were in contact to each other. We found that the biggest pigmented macromere exhibited the highest number of blastomere interactions (Fig. 3C and C′). This is consistent with the spatial positioning and number of contacts of previous suggestions for unequal (Goulding, 2003) and equal cleaving gastropods (Arnolds et al., '83). Even though we did not track the fate of each blastomere or use genetic markers to identify the potential fates of blastomeres, by using the simple criteria of the highest number of cell contacts we assigned the presumptive D macromere identity to the biggest blastomere at the four-cell stage. Nevertheless, further analyses of cell determinants and fate mapping are desired to properly identify each blastomere.

Third Cleavage Remains Asynchronous and Forms the First Quartet of Micromeres. Third cleavage was also asynchronous. Macromeres A and B divided at the same time while macromeres C and D remained undivided. As a result, a six-cell embryo was formed with two micromeres (1a and 1b) at the farthest animal side, positioned on top of the two small macromeres (Fig. 3D). Shortly after micromeres 1a and 1b completed cytokinesis at the

six-cell stage, two mitotic spindles formed in the two-pigmented macromeres C and D, which were oriented at an angle opposite to each other. The timing of cell division of C and D blastomeres occurred in asynchrony. Blastomere C completed mitosis before blastomere D (Fig. 3D′). We presume that this small asynchrony is related to the size difference of the blastomeres. By the end of this cleavage, two new micromeres formed (1c and 1d) from macromeres C and D giving rise to the eight-cell embryo. Micromeres 1c and 1d were similar in size compared to the other micromeres (1a and 1b) that originated from the A and B blastomeres. The first quartet of almost yolk-free micromeres was formed on the animal side of the embryo (Fig. 3E and E′).

Eight- to 24-Cell Stage Reveals Synchronous Divisions of Animal Micromeres in an Anticlockwise Direction. Once the embryo formed its first quartet of micromeres, small macromeres 1A and 1B divided producing two daughter cells: 2a and 2b, while the first quartet (1a–1d) and the large macromeres (C and D) remained undivided. Two new blastomeres arose (2c and 2d), one from each of the macromeres C and D, followed by cleavage of the first quartet of micromeres, which generated a new tetrad ($1a^2$, $1b^2$, $1c^2$, $1d^2$). From there on, the cleavage continued to follow the same asynchronous pattern, where the large pigmented macromeres (C and D) divided following the division of the small macromeres (A and B), producing intermediate stages of embryonic development (e.g., 10-cell stage, 11-cell stage, and so on). The tightly clustered configuration of the multicelled blastula is clearly observed from the vegetal side (Fig. 3F and F′). New yolk-free micromeres continued to arise on the animal pole of the embryo (Fig. 3G).

Gastrula Reveals the Heart-Shaped Stage. In spite of a clear proliferative activity of cells during embryogenesis, the gastrula did not substantially increase in size when compared to the embryo at its one-cell stage. Thus, the development of these cells is not accompanied by cellular growth; instead, cells decreased in size as the embryo developed and the cells divided. The first signs of cell movement in the embryo marked the beginning of gastrulation. Similar to other spiralians, gastrulation in *A. californica* occurred by epiboly (Lyons and Henry, 2014). Pigment-free micromeres migrated over the surface from the animal to the vegetal pole, surrounding other blastomeres, including the large pigmented macromeres (C and D). Due to the size of the macromeres, and the space observed between them (segmentation cavity), the gastrula became heart shaped (Fig. 3H). The general morphology of the gastrula in *A. californica* has been previously described (Heyland et al., 2011); yet, due to the autofluorescent nature of the yolk platelets and by using confocal microscopy, we have gained a better resolution of the distribution of these platelets in the embryo. We observed that the yolk platelets during the gastrula are not restricted to one pole of the embryo (Fig. 3H′). The total developmental timing from the one-cell embryo to reach the gastrula stage was 25 hr (Fig. 4).

Cytoeskeletal Dynamics. In addition to ooplasmic segregation, the orientation of the mitotic spindle seems to influence early asymmetries (Fig. 5). During the first cleavage, the mitotic spindle was not aligned perpendicularly to the animal vegetal axis of the zygote, but instead formed an angle of approximately 13° (SD = 1.27, $n = 5$; Fig. 5D) with respect to the AV axis (Fig. 5A and A′). The polarization and oblique orientation of the mitotic spindle generated differences in the distance of the centrosomes to the cortex. One aster of the mitotic spindle was located closer to the cortex (distance = 28.8 μm) compared to the other aster (distance = 16.4 μm) (Fig. 5A and A′). We also observed differences in the size of both asters during cleavage. Both of these features, that is, displacement and oblique orientation of the mitotic spindle, as well as asymmetries in size of the asters have been observed in other unequal cleaving embryos (Ren and Weisblat, 2006; Weisblat, 2007). Finally, the result of this asymmetric cleavage is a two-cell embryo with a small AB micromere positioned in an oblique orientation with respect to the big CD macromere (mean alignment angle = 38.33°, SD = 3.06, $n = 8$, Fig. 5D) (Fig. 5B and B′). After the two-cell embryo was formed, the small blastomere divided slightly earlier than the big macromere giving rise to the transient three-cell embryo. The asymmetric division of the presumptive CD macromere was evidenced by the difference in the distances from the equatorial plate to each side of the cortex (Fig. 5C and C′).

After the four-cell embryo was formed, the mitotic spindles were positioned in oblique angles with respect to the AV axis, in direction to the animal pole of the embryo, generating the first set of micromeres (1a and 1b). Later, when the embryo reached the eight-cell stage, the orientation of the spindles within the first tetrad of micromeres (1a–1d) allowed the identification of the future chirality of the embryo; our observations revealed that the micromeres in *A. californica* were displaced in an anticlockwise manner (Fig. 5E and E′), which according to studies in mollusks generates a sinistral embryo (Henley, 2012; Namigai et al., 2014). Both dextral and sinistral species have repeatedly evolved in gastropods by left–right reversal of the primary asymmetry (Vermeij, 2002; Lambert, 2010). Studies have shown that maternally inherited genes at closely linked loci (Shibazaki et al., 2004), the asymmetrical expression of nodal signaling in early embryos (Grande and Patel, 2009), and the relative orientation of the first quartet of micromeres in relation to the macromeres at the eight-cell stage embryo (Kuroda et al., 2009) determine embryo handedness.

Following the eight-cell stage, the blastomere 2b was formed in parallel to the AV axis, whereas blastomere 2a arose perpendicularly to its mother cell (Fig. 5F and F′). Later, the slight asynchrony of cleavage between blastomeres C and D produced a fleeting 11-cell stage (Fig. 5G and G) and a subsequent 12-cell stage. During this transition, the spindle axis positioned diagonally and each of the large macromeres produced a daughter

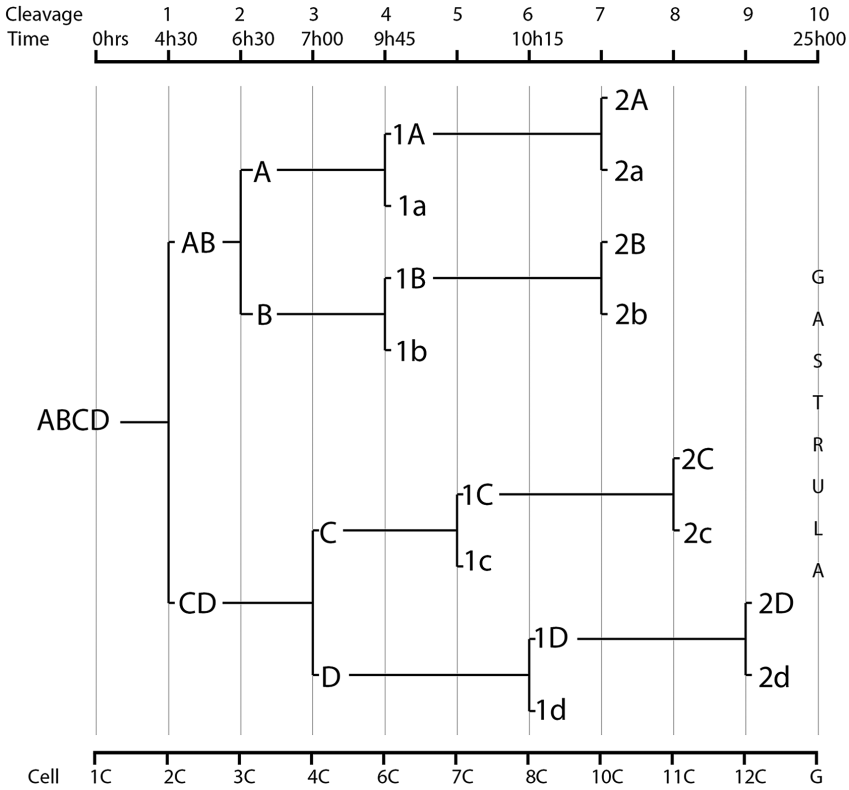

Figure 4. Early cleavage map of *Aplysia californica* showing asynchronies during development. Schematic cleavage map shows the cell lineage of the presumptive blastomeres A–D. Asynchronous cell divisions, number of cleavages, developmental timing, and number of cells during early divisions are depicted. First cleavage occurs after 4 hr and 30 min resulting in an unequal two-cell embryo with one presumptive AB blastomere and a presumptive CD blastomere. Second cleavage is asynchronous and occurs 2 hr later, only the presumptive AB blastomere divides, giving rise to a three-cell embryo. Third cleavage happens 30 min later with the division of the presumptive CD blastomere resulting in a four-cell embryo stage. Fourth cleavage occurs concomitantly in both small macromeres (presumptive blastomeres A and B). The two first small micromeres (1a and 1b) are formed from this cleavage, generating a six-cell embryo after 9 h and 45 min of development. Next cleavage occurs only at the presumptive macromere C, giving rise to the third micromere (1c) of the first quartet of micromeres. A seven-cell embryo is produced after fifth cleavage. Presumptive macromere D finally cleaves on the sixth division after 10 h and 15 min of development, completing the first tetrad of micromeres that conforms the eight-cell embryo. Later, the two macromeres A and B divide again, generating two new daughter cells (2a and 2b). During eighth cleavage, only macromere 1C divides resulting in an 11-cell embryo. The 12-cell stage is reached after division of macromere 1D that gives rise to blastomere 1d. Last stage shown here and after 25 hr of being laid, the embryo develops into a gastrula.

cell (2c and 2d, respectively) laterally oriented toward the external side of the embryo. The sinistral chirality of the embryo of *A. californica* became more evident in the blastula stages of development (Fig. 5H and H′).

Navanax aenigmaticus Early Development

Navanax aenigmaticus exhibited the stereotypical holoblastic equal cleavage found in Spiralia (Conklin, 1897). Despite the lack of pigmentation, we observed that the embryo in *N. aenigmaticus* contained a stratified cytoplasm with at least three layers of distinct contents (Fig. 6A and B′). This is consistent with previous descriptions of ooplasmic segregation during the first cleavage in the development of the congener species *Navanax inermis* (Worley and Worley, '43). As in *N. inermis*, we identified three types of ooplasmic contents: (i) albuminous yolk, (ii) fatty yolk, and (iii) animal cytoplasm. Before first cleavage, the albuminous yolk was segregated toward the lateral and vegetal regions of the embryo, while the fatty yolk, and most of the animal cytoplasm, located more centrally. The first cleavage was characterized by a symmetric cell division occurring parallel to

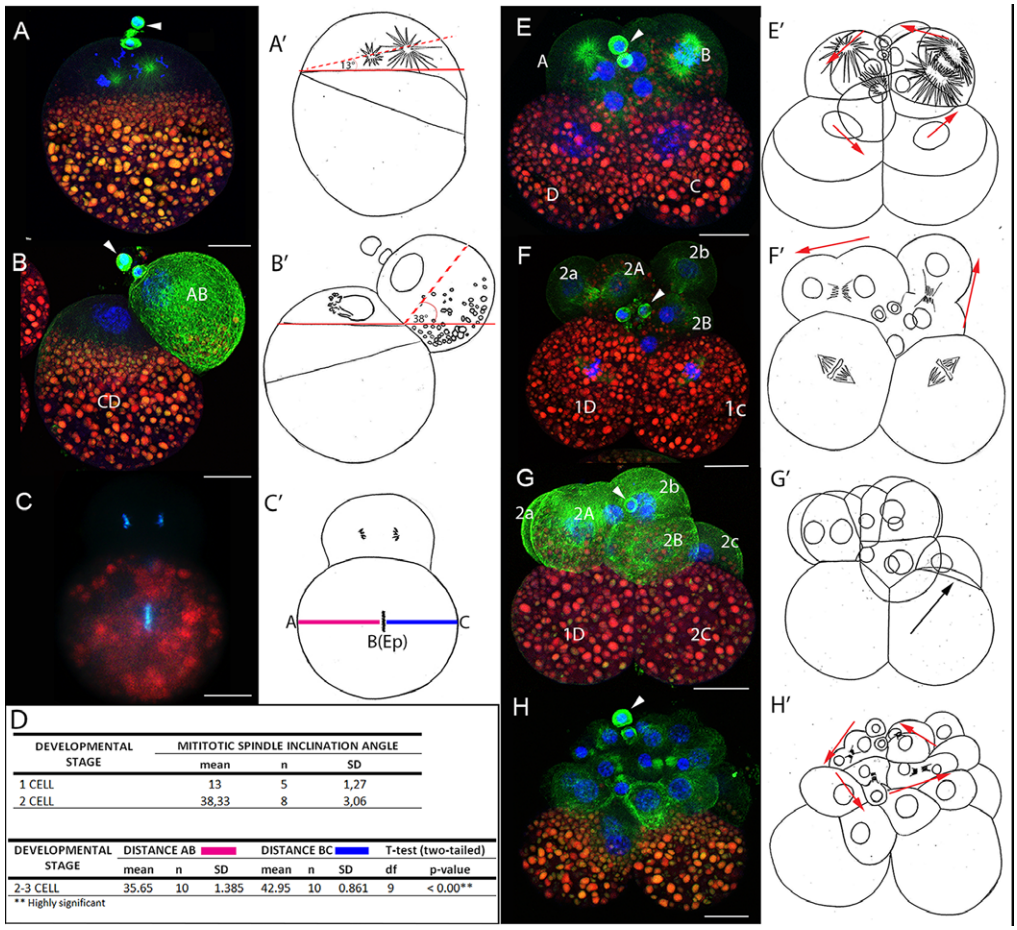

D

DEVELOPMENTAL STAGE	MITITOTIC SPINDLE INCLINATION ANGLE		
	mean	n	SD
1 CELL	13	5	1,27
2 CELL	38,33	8	3,06

DEVELOPMENTAL STAGE	DISTANCE AB			DISTANCE BC			T-test (two-tailed)	
	mean	n	SD	mean	n	SD	df	p-value
2-3 CELL	35.65	10	1.385	42.95	10	0.861	9	< 0.00**

** Highly significant

Figure 5. Dynamics of the mitotic spindle during asymmetric cell divisions in early embryos of *Aplysia californica*. (A) At one-cell stage, prior the first cleavage, the mitotic spindle is obliquely inclined. (A′) The angle of inclination of the mitotic spindle in relation to the equator of the embryo is approximately 13°. (B) Two-cell embryo. (B′) The small presumptive blastomere AB arises at an angle of 35° with respect to the equator of the presumptive CD blastomere. (C) Embryo prior the third cleavage during metaphase. (C′) A future asymmetry is evidenced by the position of the equatorial plate (Ep),which is not strictly meridional; prior the completion of the second cleavage, one of the asters is positioned closer to the cellular cortex (distance BC, blue line) compared to the other (distance AB, pink line). (D) Table showing the mean values of inclination of the angles of division, and the distance of the asters to the cortex; the results of the T-test displayed highly significant differences between the values. (E) During the eight-cell stage, the first quartet of micromeres forms in direction to the animal pole, and their size is significantly smaller than their mother cells. (E′) The first quartet of cells is displaced in an anticlockwise manner (red arrows). (F) The fourth cleavage is asynchronous and produces a 10-cell embryo. (F′) The blastomere 2b is formed parallel to the AV axis, whereas blastomere 2a arises perpendicularly. (G) An 11-cell embryo is generated through a slight asynchrony in the division of the two big macromeres (presumptive C and D). (G′) The blastomere C divides, generating a daughter 2c blastomere (black arrow). (H) 24-cell embryo. (H′) The blastomeres kept arising toward the animal pole of the embryo in a sinistral arrangement (red arrows). Polar bodies (white arrow head) are observed surrounding the animal end of the embryos from the one-cell stage until 24-cell stage. Reference line denoting the equator of the embryo (Red line). Inclination of the mitotic spindle (Red dotted line). (A′–H′) Schematic representations of (A–H). (A–H) Microtubules are shown by green immunofluorescence, nuclei by blue fluorescence, and pigmented yolk platelets by red/orange autofluorescence. (n) Number of embryos analyzed. SD, standard deviation; df, degrees of freedom. Scale bars: 20 μm. [Color figure can be viewed at wileyonlinelibrary.com]

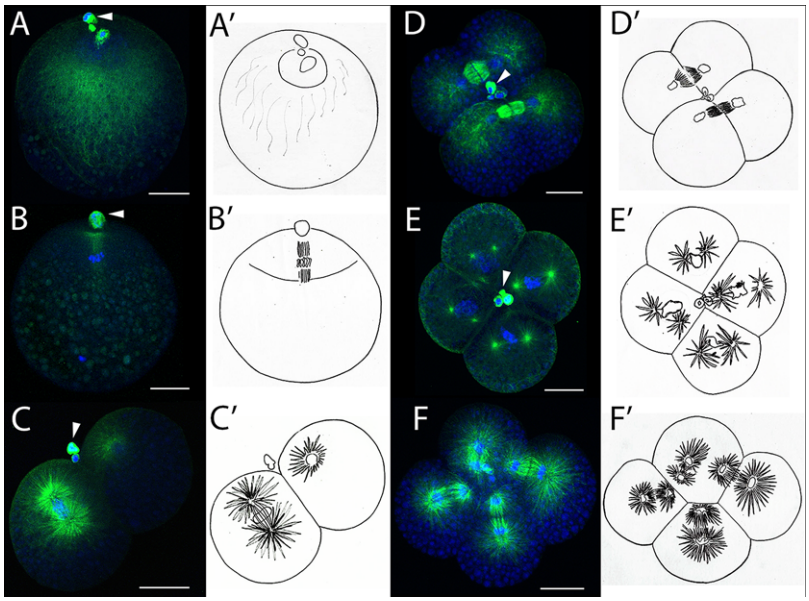

Figure 6. Stereotypical spiral cleavage exhibited by embryos of *Navanax aenigmaticus* during early development. (A) One-cell embryo depicting the reorganization of the ooplasm. (B) Stratified one-cell embryo shows three distinct contents in the cytoplasm: big yolk platelets are segregated to the vegetal and lateral sides of the zygote, whereas smaller yolk platelets remain in the center and middle regions, and a clear cytoplasm is found toward the animal pole. (C) Two-cell embryo results form a symmetrical cleavage along the AV axis. (D–F) Second cleavage is synchronous and symmetric. (D) Cytokinesis during the two- to four-cell stage transition. (E) Four-cell embryo starting to form the mitotic apparatus for the next cleavage. (F) Cytokinesis during the four- to eight-cell embryo transition. This division is synchronous and asymmetrical giving rise to the first tetrad of significantly smaller micromeres. Polar bodies (white arrow head). (A′–F′) Schematic representations of (A–F). (A–F) Microtubules are shown by green immunofluorescence, nuclei by bright blue fluorescence, and nonpigmented yolk platelets by dark blue autofluorescence of the embryos at different stages. Scale bars: 20 μm. [Color figure can be viewed at wileyonlinelibrary.com]

the AV axis, generating two equal-size blastomeres (Fig. 6C and C′), which subsequently divided producing four macromeres (A–D) without any apparent size differences (Fig. 6D and E′). During the second and third cleavages, embryogenesis occurred synchronously, and one quartet of smaller cells (micromeres) formed consecutively as a result of each cleavage (Fig 6F and F′). As observed in *A. californica* (present study), embryos of *N. aenigmaticus* exhibited an anticlockwise chirality, which translates into a further sinistral larval shell.

Comparative Analysis of Developmental Patterns in Spiralians

The phylum Mollusca presents a high diversity of cleavage types and early embryo morphology (Henry, '86; Luetjens and Dorresteijn, '98; Ren and Weisblat, 2006; Lambert, 2008, 2010; Henry et al., 2010; Lesoway et al., 2014). A feature that seems to vary substantially among mollusks is the size and arrangement of the progeny of the apical first and second tetrads/quartets of micromeres, also known as the molluskan cross (Scheltema, '93). The configuration of the molluskan cross is generally determined by the size of the micromeres in relation to their mother macromeres, but many deviations have been observed in gastropods, such as in Polyplacophora and Aplacophora (Maslakova et al., 2004), as well as in the highly divergent discoideal partial cleavage pattern of cephalopods (Boletzky, '89a, b).

Several species of spiralians are known to exhibit unequal cleavage (Henry, 2014), although equal holoblastic cleavage is generally considered a stereotypical developmental pattern of Spiralia (Wanninger, 2015). Unequal patterns of division can be generated by intracellular regulatory mechanisms involved in the organization of cytoskeletal elements, for example, the size of the asters and their distance to the cell cortex (Luetjens and Dorresteijn, '98), or by the formation of polar lobes that allow a differential deposition of cytoplasmic contents into daughter blastomeres, as has been well documented in the bivalves *Saccostrea kegaki* (Kakoi et al., 2008) and *Septifer virgatus* (Kurita et al., 2009). Polar lobes vary in size. If the lobe is large, it can generate a substantially different deposition of cytoplasmic contents into the attached macromere, as has been documented

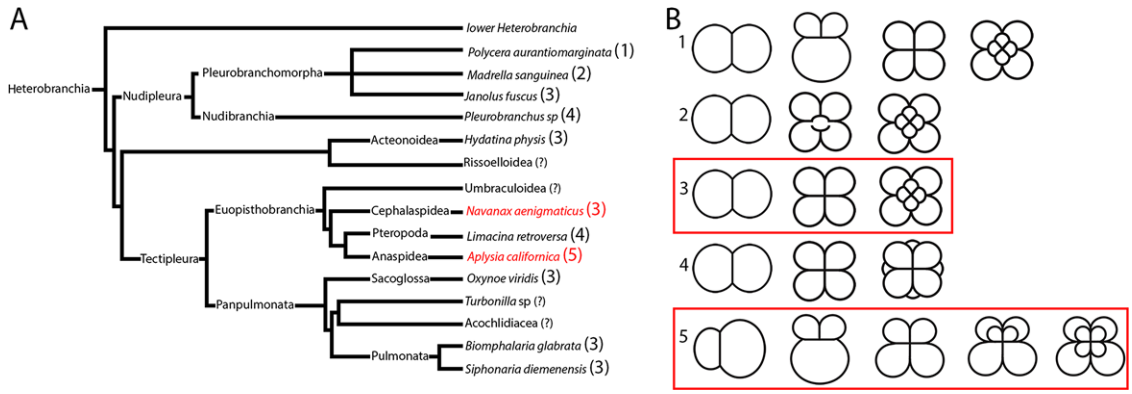

Figure 7. Recreation of the cleavage patterns observed in Heterobranchia. (A) Phylogeny based on molecular analyses of the group Heterobranchia (Zapata et al., 2014, 2015). (B) (1–5) Previously described cleavage patterns of model species are used to exemplify the high variation found within the group: *Polycera aurantiomarginata* (Martínez-Pita et al., 2006), *Madrella sanguinea* (Page, 2007), *Janolus fuscus* (Wolf and Young, 2012), *Pleurobranchus* sp. (Rao and Alagarswamy, '60), *Hydathina physis* (Hamel and Mercier, 2007), *Navanax aenigmaticus* (present study), *Limacina retroversa* (Thabet et al., 2015), *Aplysia californica* (present study), *Oxynoe viridis* (unpublished data), *Biomphalaria glabatra* (Camei and Verdonk, '70), and *Siphonaria diemensis* (Mapstone, '78). The cleavage pattern in *A. californica* noticeably differs from the rest of the group by exhibiting unequal and asynchronous early cell divisions that generate several intermediate stages, being the species that generates the highest number of cleavage rounds before reaching the eight-cell stage. (Red font) Species analyzed during this study. (Red rectangle) Cleavage patterns observed in the present study. (Black dotted circle) Polar lobe. Numbers in brackets represent the cleavage pattern exhibit by the species. [Color figure can be viewed at wileyonlinelibrary.com]

for the snail *Ilyanassa obsoleta* (Render, '89, ''91; Lambert, 2010); and if the lobe is small, it results in often unnoticeable differences in size of the macromeres, as shown for the slipper limpet *Crepidula fornicata* (Henry et al., 2010).

Recent phylogenetic analyses based on the transcriptomes of a most comprehensive list of gastropod taxa recognize the Nudipleura and Tectipleura as monophyletic groups within the Heterobranchia (Zapata et al., 2014). Within the Tectipleura, this study provides support for a Panpulmonata clade and a Euopistobranchia clade (Fig. 7). *Aplysia californica* (Anaspidea) and *N. aenigmaticus* (Cephalaspidea) belong to the Euopistobranchia clade. If we map early development patterns observed in the heterobranchs (Lalli and Conover, '73; Boring, '89; Shibazaki et al., 2004; Thabet et al., 2015) onto a current phylogeny (Zapata et al., 2014, 2015), it becomes clear that the typical equal cleavage pattern (Schaefer, '97; Soares and Calado, 2006; Wolf and Young, 2012) of the cephalaspidean *N. aenigmaticus* (present study), as well as the sacoglossan *Oxynoe viridis* (unpublished data), most parsimoniously represents the ancestral heterobranch mode of development (i.e., cleavage pattern 3 in Fig. 7).

Yet, there are heterobranchs that do not follow the norm. A pattern that seems to deviate the most from the stereotypical cleavage of heterobranchs occurs in the anaspidean *A. californica* (i.e., cleavage pattern 5 in Fig. 7). Despite of being an extensively studied model species, descriptions of *A. californica* development and its unequal cleavage pattern scarce (Saunders, '10; Raven, '58; Heyland et al., 2011; Lee et al., 2014). Detailed observations of *A. californica* development, including the formation of unequal blastomeres, heterochronic cleavage, and the presence of U- and heart-shaped embryos, demonstrate a clear deviation from other patterns observed in euopisthobranchs and heterobranchs. Remarkably, we have also observed this atypical cleavage pattern in other anaspideans such as *Stylocheilus striatus*, *Dolabrifera dolabrifera*, *Dolabella auricularia*, and *Aplysia dactylomela* (unpublished data), suggesting that this pattern of cleavage may be conserved in the Anaspidea. Previous studies of the phylogenetic relationships of opisthobranchs using morphological and molecular data have suggested that the Anaspidea may be one of the most derived clades within the group (Wägele et al., 2011; Zapata et al., 2014, 2015; Sakurai and Katz, 2015; Sevigny et al., 2015), so it is not surprising to see a most deviate pattern of cleavage in this order.

Early developmental patterns could serve as clues to elucidate future body features and processes at late stages. Several hypotheses have been postulated in order to explain the influence of different developmental traits on life histories of marine invertebrates. For example, in marine spiralians, egg size seems to be correlated to larval nutritional mode. Previous studies have shown that the allocation of cytoplasm to macromeres at the eight-cell stage embryo occurs in species with larger egg size, and this feature has been suggested to drive a delay in

the formation of a functional gut or an ultimate loss of feeding abilities in the larva, that is, lecitotrophy (Jones, 2015). In contrast, features such as small eggs (within the range of 40–170 μm in diameter), multiple embryos (up to 52 per egg capsule), large batches (within the range of 10–26 million or more per spawm-mass) and long-lived feeding larvae, as displayed by *A. californica*, are all typical characteristics of planktotrophy (Pawlik, '89; Capo et al., 2009), which has been suggested to represent the ancestral character state in most marine invertebrates (Strathmann, '78). Unfortunately, at this point of our research, we cannot associate the embryological characteristics observed in *A. californica*, such as yolk distribution and unequal cleavage, to any particular processes at late stages of development. However, based on the results obtained from previous experiments on similar unequal cleaving species (Astrow et al., '87; Lyons and Weisblat, 2009), we could presume that asymmetries and heterochronies during early cleavage must have direct implications on the developmental processes of the embryo, including differential cell communication and signaling among blastomeres, as well as D-quadrant specification and cell fate determination.

CONCLUSIONS

While unequal cleaving embryos, characterized by the formation of blastomeres of different size as a result of first and second cleavage, have been reported for several species of Anaspidea (Saunders, '10; Heyland et al., 2011; Lee et al., 2014); yet, this study reveals in great cellular detail six previously unknown mechanisms of development involved in generating the peculiar unequal cleavage of *A. californica*: (i) cytoplasmic rearrangement and ooplasmic segregation generating a temporarily U-shaped embryo; (ii) differences in the size of the two asters and their proximity to the cortex; (iii) oblique orientation of the mitotic spindle during first cleavage; (iv) slight asynchrony between the cleavage timing of the two large macromeres (C and D) that results in odd numbers of cells during intermediate stages (e.g., three- or 11-cell stage); (vi) distribution of yolk platelets outside large macromeres during the heart-shaped gastrula, showing a particularly high concentration of platelets at the presumptive posterior end of the embryo. We observed a relationship between the position of cytoskeletal elements to the site of first invagination of the cleavage furrow, as well as a relationship between the orientation of the mitotic spindle to the direction of the invaginating furrow. Further research is needed to reveal how the novel cellular interactions and dynamics observed in *A. californica* unequal cleavage influence cell fates, axis determination, or larval phenotypes.

Patterns of early development vary substantially in the Euopisthobranchia, as well as in the Heterobranchia. By mapping early cleavage patterns of several Heterobranchs on current transcriptomic phylogenies, we propose that an equal and synchronous cleavage is the ancestral state of the Heterobranchia, whereas the peculiar unequal cleavage observed in *A. californica* and other Anaspidea is highly derived. Future research should address the evolutionary implications and adaptive significance of unequal cleavers.

ACKNOWLEDGMENTS

This study was funded by collaboration between the Pontificia Universidad Católica del Ecuador and Universidad de Los Andes in Colombia. F.D.B. was supported by an Assistant Professor Grant from Universidad de los Andes and a Prometeo Research Award from the Secretaría Nacional de Ciencia, Tecnología e Innovación (Senescyt-Ecuador). We would like to thank María Herminia Cornejo, Richard Strathmann, and Fernanda Oyarzun for the initial encouragement to pursue this study during the "Embryo and Larvae Course" that took place at the CENAIM-ESPOL, San Pedro (Prov. of Santa Elena) in 2012. We would like to specially thank Denisse Galarza Verkovitch for her research support. Her involvement in the setting up and maintaining of assays was invaluable and essential for the success of this research project. We are grateful to Miss Stefania Tapia for her assistance during the preparation of samples. Finally, we would like to thank Stefania Gutierrez and Olga Lucía Torres for their help and support during image processing at Universidad de Los Andes in Bogotá.

LITERATURE CITED

Adell T, Martín-Durán JM, Saló E, Cebrià F. 2015. Platyhelminthes. In: Wanninger A, editor. Evolutionary developmental biology of invertebrates 2. Wien, Austria: Springer. p 21–40.

Arnolds WJA, van den Biggelaar JAM, Verdonk NH. 1983. Spatial aspects of cell interactions involved in the determination of dorsoventral polarity in equally cleaving gastropods and regulative abilities of their embryos, as studied by micromere deletions in Lymnaea and Patella. Roux Arch Dev Biol 192:75–85.

Astrow S, Holton B, Weisblat D. 1987. Centrifugation redistributes factors determining cleavage patterns in leech embryos. Dev Biol 120:270–283.

Bandel K. 1976. Egg Masses of 27 Caribbean opisthobranchs from Santa Marta, Columbia. Stud Neotrop Fauna E 11:87–118.

Benkendorff K, Davis R, Bremner JB. 2001. Chemical defense in the egg masses of benthic invertebrates: an assessment of antibacterial activity in 39 mollusks and 4 polychaetes. J Invertebr Pathol 78:109–118.

Bleidorn C, Helm C, Weigert A, Aguado MT. 2015. Annelida. In: Wanninger A, editor. Evolutionary developmental biology of invertebrates 2. Wien, Austria: Springer. p 1–289.

Boletzky SV. 1989a. Recent Studies on spawning, embryonic development, and hatching in the Cephalopoda. Adv Mar Biol 25:85–115.

Boletzky SV. 1989b. Early ontogeny and evolution: the cephalopod model viewed from the point of developmental morphology. Geobios 22:67–78.

Boring L. 1989. Cell-cell interactions determine the dorsoventral axis in embryos of an equally cleaving opisthobranch mollusc. Dev Biol 136:239–253.

Camacho-Garcia Y, Gosliner T, Valdés A. 2005. Guía de Campo de las Babosas Marinas del Pacífico Este Tropical (California). San Francisco, CA: California Academy of Sciences. p 61.

Camei T, Verdonk NH. 1970. The early development of the snail *Biomphalaria glabrata*. Neth J Zool 10:93–121.

Canman JC. 2009. Cytokinetic astralogy. J Cell Biol 187:757–759.

Capo TR, Bardales AT, Gillete PR, et al. 2009. Larval growth, development, and suvival of laboratory *Aplysia californica*: effects of diet and veliger density. Comp Biochem Physiol 149:215–223.

Chia F, Gibson G, Qian P. 1996. Poecilogony as a reproductive strategy of marine invertebrates. Oceanol Acta 19:203–208.

Clement AC. 1952. Experimental studies on germinal localization in Ilyanassa. I. The role of the polar lobe in determination of the cleavage pattern and its influence in later development. J Exp Zool Part B 121:593–625.

Conklin EG. 1897. The embryology of Crepidula. J Morph 13:1–226

Costello P, Henley C. 1976. Spiralian development: a perspective. Am Zool 291:277–291.

Croll RP. 2006. Development of embryonic and larval cells containing serotonin, catecholamines, and FMRFamide-related peptides in the gastropod mollusc Phestilla sibogae. Biol Bull 211:232–247.

D'Avino PP, Savoian MS, Glover DM. 2005. Cleavage furrow formation and ingression during animal cytokinesis: a microtubule legacy. J Cell Sci 118:1549–1558.

Dohmen MR. 1983. The polar lobe in eggs of molluscs and annelids: structure, composition, and function. In Jeffery W, Raff R, editors. Time, space and pattern in embryonic development. vol 2. New York: A. R. Liss Inc. p 197–220.

Dzik J. 1999. Evolutionary origin of asymmetry in early metazoan animals. In: Pályi G, Zucchi C, Caglioti L, editors. Advances in BioChirality. Amsterdam: Elsevier Science. p 153–190.

Freeman G. 2006. Oocyte and egg organization in the patellogastropod Lottia and its bearing on axial specification during early embryogenesis. Dev Biol 295:141–155.

Freeman G, Lundelius JW. 1992. Evolutionary implications of the mode of D quadrant specification in coelomates with spiral cleavage. J Evol Biol 5:205–247.

Gilbert SF. 2014. Early development in vertebrates, Chapter 9: birds and mammals. In: Gilbert SF, editor. Developmental biology, 10th edition. Sunderland, MA : Sinauer Associates, Inc. p 301–302.

Glotzer M. 2004. Cleavage furrow positioning. J Cell Biol 164:347–351.

Goldstein B, Freeman G. 1997. Axis specification in animal development. BioEssays 19:105–116.

Goulding M. 2003. Cell contact-dependent positioning of the D cleavage plane restricts eye development in the Ilyanassa embryo. Development 130:1181–1191.

Grande C, Patel NH. 2009. Nodal signalling is involved in left-right asymmetry in snails. Nature 457:1007–1011.

Hamel JF, Mercier A. 2007. Development and movement of the opisthobranch, *Hydatina physis*, in the in the Solomon Islands. SPC Trochus Inf Bull 13:19–24.

Hejnol A. 2010. A twist in time—the evolution of spiral cleavage in the light of animal phylogeny. ICB 50:695–706.

Henley CL. 2012. Possible origins of macroscopic left-right asymmetry in organisms. J Stat Phys 148:740–774.

Henry JJ. 1986. The role of unequal cleavage and the polar lobe in the segregation of developmental potential during first cleavage in the embryo of *Chaetopterus variopedatus*. Roux Arch Dev Biol 195:103–116.

Henry JQ. 2014. Spiralian model systems. Int J Dev Bio 58:389–401.

Henry JJ, Martindale MQ. 1999. Conservation and innovation in spiralian development. Hydrobiologia 402:255–265.

Henry JQ, Perry KJ, Martindale MQ. 2006. Cell specification and the role of the polar lobe in the gastropod mollusc *Crepidula fornicata*. Dev Biol 297:295–307.

Henry JJ, Collin R, Perry KJ. 2010. The slipper snail, Crepidula: an emerging lophotrochozoan model system. Biol Bull 218:211–229.

Heyland A, Vue Z, Voolstra CR, Medina M, Moroz LL. 2011. Developmental transcriptome of *Aplysia californica*. J Exp Zool Part B:316:113–134.

Jackson DJ, Degnan M, Degnan M. 2012. Variation in rates of early development in *Haliotis asinina* generate competent larvae of different ages. Fronts Zool 9:1–9.

Jones C. 2015. Evolutionary changes in development associated with a transition in larval nutritional mode in spiralians [MSc thesis]. Long Beach: California State University.

Kakoi S, Kin K, Miyazaki K, Wada H. 2008. Early development of the Japanese spiny oyster (*Saccostrea kegaki*): characterization of some genetic markers. Zool Sci 25:455–464.

Kaviarasan T, Siva SR, Yogamoorthi A. 2012. Antimicrobial secondary metabolites from marine gastropod egg capsules and egg masses. Asian Pac J Trop Biomed 2:916–922.

Klussmann-Kolb A, Wagele H. 2001. On the fine structure of opisthobranch egg masses (Mollusca, Gastropoda). Zool Anz 240:101–118.

Krug PJ. 1998. Poecilogony in an estuarine opisthobranch: planktotrophy, lecithotrophy, and mixed clutches in a population of the ascoglossan *Alderia modesta*. Mar Biol 132:483–494.

Kurita Y, Deguchi R, Wada, H. 2009. Early development and cleavage pattern of the Japanese purple mussel, *Septifer virgatus*. Zool Sci 26:814–820.

Kuroda R, Endo B, Abe M, Shimizu M. 2009. Chiral blastomere arrangement dictates zygotic left-right asymmetry pathway in snails. Nature 462:790–794.

Lalli CM, Conover RJ. 1973. Reproduction and development of *Paedoclione doliiformis*, and a comparison with *Clione limacina* (Opisthobranchia: Gymnosomata). Mar Biol 19:13–22.

Lambert, JD. 2008. Mesoderm in spiralians: the organizer and the 4d cell. J Exp Zool Part B 310:15–23.

Lambert JD. 2010. Developmental patterns in Spiralian embryos. Curr Biol 20:R72–R77.

Lee C, Kaang B, Lee Y. 2014. Spawning behavior and egg development of *Aplysia kurodai* inhabiting the coastal waters of Jeju Island, Korea. Dev Reprod 18:25–31.

Lesoway MP, Abouheif E, Collin R. 2014. The development of viable and nutritive embryos in the direct developing gastropod *Crepidula navicella*. Int J Dev Biol 58:601–611.

Luetjens CM, Dorresteijn AW. 1998. Dynamic changes of the microtubule system corresponding to the unequal and spiral cleavage modes in the embryo of the zebra mussel, *Dreissena polymorpha* (Mollusca, Bivalvia). Zygote 6:239–248.

Lyons DC, Henry JQ. 2014. Ins and outs of spiralian gastrulation.Int J Dev Biol 58:413–428.

Lyons DC, Weisblat DA. 2009. D quadrant specification in the leech Helobdella: actomyosin contractility controls the unequal cleavage of the CD blastomere. Dev Biol 334:46–58.

Mapstone GM. 1978. Egg capsules and early development in *Siphonaria diemenensis* (Quoy & Gaimard, 1833) and *Siphonaria baconi* (Reeve,1856). J Malac Soc Aust 4:85–92.

Martindale MQ. 1986. The organizing role of the D quadrant in an equal-cleaving spiralian, *Lymnaea stagnalis* as studied by UV laser deletion of macromeres at intervals between 3rd and 4th quartet formation. Int J Invertebr Repr Dev 9:229–242.

Martínez-Pita I, Sánchez-España AI, García FJ. 2006. Some aspects of the reproductive biology of two Atlantic species of Polycera (Mollusca: Opisthobranchia). J Mar Biol Ass UK 86:391.

Maître JL, Niwayama R, Turlier H, Nédélec F, Hiiragi T. 2015. Pulsatile cell-autonomous contractility drives compaction in the mouse embryo. Nat Cell Biol 17:849–855.

Maslakova SA, Martindale MQ, Norenburg JL. 2004. Fundamental properties of the spiralian developmental program are displayed by the basal nemertean *Carinoma tremaphoros* (Palaeonemertea, Nemertea). Dev Biol 267:342–360.

Namigai EKO, Kenny NJ, Shimeld SM. 2014. Right across the tree of life: the evolution of left-right asymmetry in the Bilateria. Genesis 52:458–470.

Ornelas-Gatdula E, Camacho-García Y, Schrödl M, et al. 2012. Molecular systematics of the "*Navanax aenigmaticus*" species complex (Mollusca, Cephalaspidea): coming full circle. Zool Scr 41:374–385.

Page LR. 2007. Novel embryogenesis in a nudibranch gastropod: segregation, expulsion, and abandonment of deeply pigmented egg cytoplasm. Biol Bull 213:303–306.

Palmer AR. 1996. From symmetry to asymmetry: phylogenetic patterns of asymmetry variation in animals and their evolutionary significance. Proc Natl Acad Sci USA 93:14279–14286.

Pawlik JR. 1989. Larvae of the sea hare *Aplysia californica* settle and metamorphose on an assortment of macroalgal species. Mar Ecol-Prog Ser 52:195–199.

Przeslawski R. 2004. Chemical sunscreens in intertidal gastropod egg masses. Invertebr Reprod Dev 46:119–124.

Rao KV, Alagarswamy K. 1960. External morphology and early development of Pleurobranchus (Oscanius) sp. from gulf of Mannar. J Mar Biol Ass India 3:255–259.

Raven CP. 1958. Chapter I. Oogenesis: vitellogenesis. In Raven CP, editor. Morphogenesis: the analysis of molluscan development. Great Britain: Pergamon Press Ltd. p 12–14.

Ren X, Weisblat DA. 2006. Asymmetrization of first cleavage by transient disassembly of one spindle pole aster in the leech *Helobdella robusta*. Dev Biol 292:103–115.

Render J. 1989. Development of *Ilyanassa obsoleta* embryos after equal distribution of polar lobe material at first cleavage. Dev Biol 132:241–250.

Render J. 1991. Fate maps of the first quartet micromeres in the gastropod *Ilyanassa obsoleta*. Development 113:495–501.

Sakurai A, Katz PS. 2015. Phylogenetic and individual variation in gastropod central pattern generators. J Comp Physiol A 201:829–839.

Sandenbergh L, Roodt-Wilding R. 2012. Investigation of the autofluorescence of various abalone (*Haliotis midae*) tissues and the implications for future use of fluorescent molecules. J Shellfish Res 31:785–788.

Saunders A. 1910. The development of *Aplysia punctata*. Q J Microsc Sci 55:497–539.

Schaefer K. 1997. Early development and morphogenesis of the intracapsular veliger of *Haminaea navicula* (Gastropoda: Opisthobranchia: Bullomorpha). Invertebr Reprod Dev 32:89–105.

Scheltema AH. 1993. Aplacophora as progenetic aculiferans and the coelomate origin of mollusks as the sister taxon of Sipuncula. Biol Bull 184: 57–78.

Sevigny JL, Kirouac LE, Thomas WK, et al. 2015. The mitochondrial genomes of the Nudibranch Mollusks, *Melibe leonina* and *Tritonia diomedea*, and their impact on Gastropod phylogeny. PlosOne 10:1–21.

Shibazaki Y, Shimizu M, Kuroda R. 2004. Body handedness is directed by genetically determined cytoskeletal dynamics in the early embryo. Curr Biol 14:1462–1467.

Shimizu T, Nakamoto A, Nakamoto A. 2014. Developmental significance of D quadrant micromeres 2d and 4d in the oligochaete annelid *Tubifex tubifex*. Int J Dev Biol 58:445–456.

Soares C, Calado G. 2006. Spawn and early development of two sympatric species of the genus Doriopsilla (Opisthobranchia: Nudibranchia) with contrasting developmental strategies. Rec West Aust Mus 69:103–109.

Strathmann RR. 1978. The evolution and loss of feeding larval stages of marine invertebrates. Evolution 32:894–906.

Thabet AA, Maas AE, Lawson GL, Tarrant AM. 2015. Life cycle and early development of the thecosomatous pteropod *Limacina retroversa* in the Gulf of Maine, including the effect of elevated CO_2 levels. Mar Biol 162:2235–2249.

Van den Biggelaar J, Haszprunar G. 1996. Cleavage patterns and mesentoblast formation in the Gastropoda: an evolutionary perspective. Evolution 50:1520–1540.

Vermeij GJ. 2002. Characters in context: molluscan shells and the forces that mold them. Paleobiology 28:41–54.

Von Dassow G, Verbrugghe KJC, Miller AL, Sider JR, Bement WM. 2009. Action at a distance during cytokinesis. J Cell Biol 187:831–845.

Von Döhren. 2015. Nemertea. In: Wanninger A, editor. Evolutionary developmental biology of invertebrates 2. Wien, Austria: Springer. p 155–192.

Vue Z, Kamel BS, Capo TR, Bardales AT, Medina M. 2014. Comparative analysis of early ontogeny in *Bursatella leachii* and *Aplysia californica*. Peer J 2:e700.

Wägele H. 1996. On egg clutches of some antarctic Opisthobranchia. Malacol Rev 28:21–30.

Wägele H, Deusch O, Händeler K, et al. 2011. Transcriptomic evidence that longevity of acquired plastids in the photosynthetic slugs *Elysia timida* and *Plakobranchus ocellatus* does not entail lateral transfer of algal nuclear genes. Mol Biol Evol 28:699–706.

Wanninger A, Wollesen T. 2015. Mollusca. In: Wanninger A, editor. Evolutionary developmental biology of invertebrates 2. Wien, Austria: Springer. p 103–154.

Weisblat DA. 2007. Asymmetric cell divisions in the early embryo of the leech *Helobdella robusta*. Prog Mol Subcell Biol 45:77–94.

Wilson NG. 2002. Egg masses of *Chromodoris nudibranchs*. Malacologia 44:289–305.

Wolf M, Young CM. 2012. Complete development of the northeast pacific *Arminacean nudibranch Janolus fuscus*. Biol Bull 222:137–149.

Worley LG, Worley EK. 1943. Studies of the supravitally stained Golgi apparatus. I. Its cycle in the tectibranch mollusc, *Navanax inermis* (Cooper). J Morphol 73:365–399.

Yin Z, Zhu M, Tafforeau P, et al. 2013. Early embryogenesis of potential bilaterian animals with polar lobe formation from the Ediacaran Weng'an biota, South China. Precambrian Res 225:44–57.

Zapata F, Wilson NG, Howison M, Andrade SCS, Jörger KM, Schrödl M, Goetz FE, Giribet G, Dunn CW. 2014. Phylogenomic analyses of deep gastropod relationships reject Orthogastropoda. Proc R Soc B 281:20141739 (1–9).

Zapata F, Wilson NG, Howison M, et al. 2015. Correction to phylogenomic analyses of deep gastropod relationships reject Orthogastropoda. Pro R Soc B 282:1802.